

Signatures of fractional Hall quasiparticles in moments of current through an antidot

Alessandro Braggio¹, Nicodemo Magnoli², Matteo Merlo^{1,2}, and Maura Sassetti¹¹Dipartimento di Fisica, INFN-LAMIA, Università di Genova,
Via Dodecaneso 33, I-16146 Genova, Italy²Dipartimento di Fisica, INFN, Università di Genova,
Via Dodecaneso 33, I-16146 Genova, Italy

(Dated: February 8, 2022)

The statistics of tunneling current in a fractional quantum Hall sample with an antidot is studied in the chiral Luttinger liquid picture of edge states. A comparison between Fano factor and skewness is proposed in order to clearly distinguish the charge of the carriers in both the thermal and the shot limit. In addition, we address effects on current moments of non-universal exponents in single-quasiparticle propagators. Positive correlations, result of propagators behaviour, are obtained in the shot noise limit of the Fano factor, and possible experimental consequences are outlined.

PACS numbers: 73.23.-b, 72.70.+m, 73.43.Jn

Introduction – The properties of quasiparticles in the fractional quantum Hall effect (FQHE) have received great attention since Laughlin's work for the states at filling factor $\nu = 1/p$; p odd integer, in which gapped bulk excitations were predicted to exist and to possess fractional charge $e^* = e$ (e = electron charge) [1]. A theory of the FQHE in terms of edge states has been proposed by Wen [2]. This theory recovered the fractional numbers of quasiparticles in the framework of chiral Luttinger Liquids (LL), and indicated tunneling as an accessible tool to probe them [3]. A charge $e^* = 3$ of quasiparticles in the $\nu = 1/3$ state was indeed measured in shot noise experiments with point-contact geometries and edge-edge backscattering [4]. In addition, LL theory predicts a universal interaction parameter equal to $\alpha = 1$. The resulting edge tunneling density of states should reflect in a power-law behaviour of I – V curves with universal exponents, e.g. $I \propto V^{\alpha+1}$ in the case of metal-edge tunneling [3]. Experiments with edge states at filling $\nu = 1/3$ indeed proved a power-law behaviour but with an exponent different from 3 [5], and deviations were observed also in the point contact geometry [4, 6]. The disagreement of LL predictions with observed exponents is still not completely understood, although several mechanisms have been put forward, including coupling to phonons [7, 8], interaction with reservoirs [9], and edge reconstruction with smooth confining potentials [10].

In this Letter, we aim to find signatures of fractional charge in different transport regimes, and to distinguish them from effects due to quasiparticle propagators. We consider a system consisting in a quantum Hall sample with an embedded antidot (Fig. 1(a)) at filling factor $\nu = 1/p$. We derive unambiguous signatures of the fractional charge in processes with different transport statistics through a comparison of noise and skewness in the sequential regime. In addition, we find transport regimes where the Fano factor is sensitive to the power laws of the quasiparticle propagators and presents super-poissonian

correlations. The peculiar behaviour driven by the quasiparticles could allow for a direct estimate of possible renormalization effects in propagators. The choice of the system has been motivated by recent experiments [11] on fractional charge and statistics. These geometries seem indeed a promising candidate to verify experimentally our predictions.

Model – Edge states form at the boundaries of the sample and around the antidot (Fig. 1(a)); tunneling barriers couple the antidot with both edges. The Hamiltonian reads $H = H_L^0 + H_R^0 + H_A^0 + H^{AB} + H_L^T + H_R^T$, where the H_i^0 are Wen's Hamiltonians for the left, right and antidot edge ($i = L; R; A$), $H^{AB} = \frac{1}{2} \sum_{\alpha} A_{\alpha} \hat{j}_{\alpha}$ describes the coupling of the antidot current \hat{j}_{α} with the vector potential A_{α} , and H_i^T is the tunneling between the $i = L; R$ infinite edges and the antidot. With $\hbar = 1$, one has [12]

$$H_L^0 = \frac{v}{4} \int dx (\partial_x \phi_L(x))^2; \quad (1)$$

where v is the edge magnetoplasmon velocity and $\phi_i(x)$ are scalar fields satisfying the equal-time commutation relations $[\phi_i(x); \phi_j(x^0)] = i \delta_{ij} \text{sgn}(x - x^0)$ whose sign depends on the chirality. For the antidot of length L , the field $\phi_A(x)$ comprises a zero-mode describing the charged excitations and a neutral boson satisfying periodic boundary conditions, $H_A^0 = E_c n^2 + \sum_{\alpha} \int_0^L dx \frac{1}{2} \dot{a}_{\alpha}^2$. Here, $E_c = \frac{1}{2} v^2 L$ is the topological charge excitation energy, and n is the excess number of elementary quasiparticles; for the neutral sector, a_{α} and a_{α}^{\dagger} are bosonic operators (plasmons) and $\omega_{\alpha} = 2\pi v/L$ is the plasmonic excitation energy [12]. The effect of H^{AB} is merely to shift the energies in H_A^0 according to $E_c n^2 \rightarrow E_c (n - \frac{1}{2})^2$, where $\frac{1}{2} = \frac{1}{2} \oint dx \frac{1}{2\pi} \partial_x \phi_A$ is the Aharonov-Bohm flux through the antidot measured in $\Phi_0 = hc/e$ [12].

The term $H^T = \sum_{i=L,R} t_i \sum_{\alpha} \int_0^L dx \psi_{\alpha}^{\dagger}(x) \psi_{\alpha}(x) + \text{h.c.}$ represents the most relevant processes of single-quasiparticle tunneling [3, 12]. Here, $\psi_{\alpha}^{\dagger}(x) / \psi_{\alpha}(x)$ are the creation operators for quasiparticles in the leads and in the antidot. Standard commutation relations ensure a charge

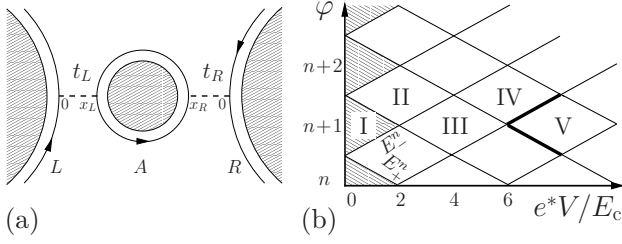


FIG. 1: (a) Geometry of the system. (b) Scheme of transport regions in the $(V'; E^n)$ plane. Roman numbers indicate the number of charge states involved in the transport – hatched, blockade regions. Thin lines signal the onset of transitions, where energies $E^n = 0$ (see text). Thick lines indicate the diamond where plasmonic excitations first enter into effect for $n=1, 3$ (region V).

of quasiparticles $e = e/2$). The tunneling probability ratio between the two barriers is tuned by an asymmetry $t_R/t_L = J_R/J_L$. A source-drain voltage V is applied between the left and right edges, producing a backscattering tunneling current of quasiparticles through the antidot $I(t) = [I_L(t) - I_R(t)]/2$, with $(j = L, R)$

$$I_j(t) = ie \int_{-\infty}^t dx_j(t) - j(0; t) \quad (2)$$

Sequential tunneling rates – For sufficiently small tunneling as compared with temperature, transport can be safely described within the sequential tunneling regime [13]. Here, the main ingredients are the incoherent tunneling rates $\Gamma_{L,R}(E)$. Their expression is well known within the Luttinger description of edge states with fully relaxed plasmonic excitations of the antidot [14, 15]. One has $\Gamma_{\pm}(E) = J_{\pm}^2(E) = J_{\pm}^2 w_1(E)$ where E is the energy associated to the quasiparticle tunneling event and $w_1(x) = (1/2)^{1/g} \Gamma(g+1/2) e^{-x/2}$ with (x) the Euler Gamma function and $\beta = 1/k_B T$. The factors w_1 are function of the plasmonic energy ϵ , the interaction parameter g and the cut-off energy ϵ_c [15]. Note that in the standard LL theory $g = 1$. Here, we will assume $g = F$ in order to describe possible renormalization effects due to coupling of the infinite edges with additional modes, e.g. phonons, or to edge reconstruction. The explicit value of F will depend on the details of interaction [7, 8, 9, 10] and here we will consider it as a free parameter. Note also that the fractional charge e is solely determined by F and is thus separated from the dynamical behaviour governed by g .

For $g < 1$ the rates scale at low temperatures as T^{g-1} at energy $E = 1$. This behaviour is reflected in the increase of the linear conductance maximum G_{max}/T^{g-2} with decreasing temperature. In order to be consistent with the tunneling approximation we then require $G_{max} e^2 = h$, setting a limit to the low temperature regime [13].

Moments – Hereafter, we will study higher current mo-

ments as a tool to determine the LL exponent [9] and the carrier charge, decoupling the latter from the information on the statistics of the transport process. We will consider the n -th order normalized current cumulant [16],

$$k_n = \frac{h I_i^n}{I_i^n h I_i^n} \quad (3)$$

Here, $h I_i$ is the stationary current and $h I_i^n = \lim_{t \rightarrow \infty} (e)^n h N_i^n =$ is the n -th irreducible current moment given in terms of the irreducible moments of the number N of charge e particles transmitted in the time t . Fano factor and normalized skewness correspond to $k_{2,3}$.

The statistics of a transport process is completely identified by its cumulants $h N_i^n$. Indeed, if a process with a given statistics takes place at different filling factors with $e_1 = e_1 e$ and $e_2 = e_2 e$, then the comparison of the n -th order current cumulants gives direct information on the charge ratio according to $k_n(e_1) = k_n(e_2) = (e_1/e_2)^{n-1}$ [17]. We suggest to revert this approach to detect the charge fractionalization in our antidot geometry. To do so, we define special the conditions in the parameter space where our system has the same transport statistics for different filling factors and independently from the value of g [18]. Note that a comparison of all moments would be required to identify special regimes. Here, we will adopt only the minimal comparison of the second and third moment that are more accessible in experiments. Furthermore, unlike simpler geometries our system offers the possibility to identify several special points with different statistics by changing external parameters.

The detailed analysis of $k_{2,3}$ is obtained directly from the cumulant generating function calculated in the Markovian master equation framework [19] in the sequential regime. The stationary occupation probability of a fixed number of antidot quasiparticles is obtained in analogy to the electron number occupation in quantum dots [14]. Assuming a symmetric voltage drop at the barriers, the change in energy for the forward transitions $n \rightarrow n+1$, $n+1 \rightarrow n$ is $E^n = eV/2 \pm 2E_c$ ($n=1, 2$) respectively. The conditions $E^n = 0$ grid the $(V'; E^n)$ plane into diamonds according to the scheme in Fig. 1(b).

Results – We focus at first on the few-state regime $eV < 2E_c$. In regions I transport is suppressed; linear conductance oscillations exist in regions I, II with a periodicity of a flux quantum ϕ_0 for any F , in accordance with gauge invariance [20]. In the same regime, an analytical treatment of $k_{2,3}$ is possible. Since the energy spectrum is periodic in V' , we start at $n = 0$. Here the forward tunneling rates $\Gamma^0 = \Gamma(E^0)$ dominate the dynamics and we recover a known formula [15, 21] for the Fano factor

$$\frac{k_2}{k_1} = \coth\left(\frac{eV}{2}\right) + 2 \frac{f(eV)}{f_{tot}} \quad (4)$$

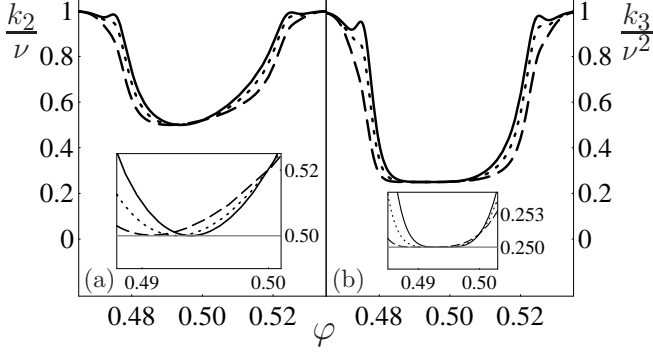


FIG. 2: Shot noise limit with $g = 1.5$, $eV = 0.1E_c$, $k_B T = 0.004E_c$ and different $g = 1=5$ (solid), $g = 1=3$ (dotted), $g = 1=2$ (dashed). (a) Fano factor $k_2 =$ and (b) skewness $k_3 =$ vs. magnetic flux ϕ . Insets: zoomed regions of the minima, with grey lines at (a) $1/2$ and (b) $1/4$.

where $\text{tot} = \int_0^\infty f_+(E_+^0) + \int_0^\infty f_-(E_-^0)$ with $f(x) = 1 - e^{-x}$.

For the skewness we find

$$\frac{k_3}{2} = 1 - 6 \frac{\int_0^\infty f_+(eV)}{\text{tot}^2} + 12 \frac{\int_0^\infty f_+^2(eV)}{\text{tot}^4} : (5)$$

We analyze now the behaviours (4) and (5) varying the ratio $eV = k_B T$.

Shot noise limit $k_B T \ll eV$. In the blockade regions I with $j E^0 j = 1$, one has $k_2 =$ and $k_3 =$. In this case the statistics of the transport process is poissonian: the transport through the antidot is almost completely suppressed, $I \approx 0$, and the residual current is generated only by a thermally activated tunneling that is completely uncorrelated. So in region I for a fixed value of filling factor, $k_{2,3}$ take maximal values corresponding to a poissonian transport process, thus constituting an example of special regime.

We consider the two-state regime (II) for $E^0 = 1$. For fractional edges $g < 1$, $k_{2,3}$ have a particular functional dependence on ϕ . We find that they both develop a minimum [22] and that the absolute values of the minima are, respectively, $k_2^{\text{min}} = 2$ and $k_3^{\text{min}} = 4$. These minimal values do not depend on g , as the comparison of solid ($g = 1=5$), dotted ($g = 1=3$) and dashed ($g = 1=2$) curves in Fig. 2 confirms. For Fermi liquid edges $g = 1$, we have $k_2 = (1 + \gamma^2)/(1 + \gamma^2)$ and $k_3 = 1 - 6(1 + \gamma^2)/(1 + \gamma^4)$ independently from ϕ . Here, k_2 and k_3 assume their minimal values $=2$ and $=4$ in the symmetric case $\gamma = 1$. In this conditions we have the strongest anticorrelation that is signalled by a marked sub-poissonian statistics.

We can conclude that in the two-state regime, in the shot noise limit, the values of the minima for $k_{2,3}$ obtained varying ϕ correspond to a special condition where the system shows the same sub-poissonian statis-

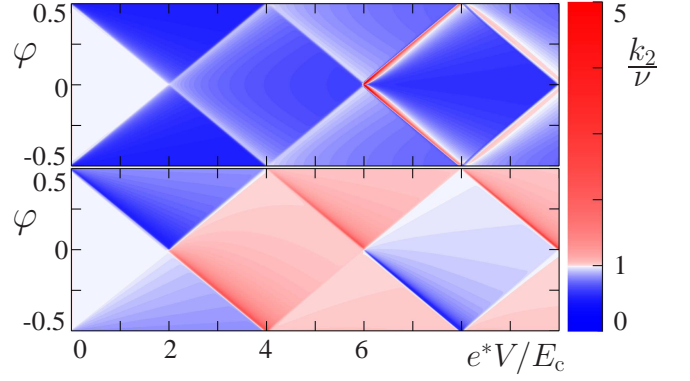


FIG. 3: Fano factor $k_2 =$ at $g = 1=3$, $k_B T = 0.01E_c$, vs. source-drain voltage and magnetic flux. Top panel: symmetric barriers $\gamma = 1$. Bottom panel: strong asymmetry $\gamma = 10$. Right panel: color scale.

tics (strongest anticorrelation) for any $g \geq 1$.

In the intermediate regime $eV \sim k_B T$, $k_{2,3}$ depend more strongly on the parameter g , and the interplay of two energy scales prevents the onset of special regimes.

Thermal regime $eV \sim k_B T$. In this limit the Fano factor is independent from the charge fractionalization, $k_2 = 2k_B T = eV$, reflecting the fluctuation-dissipation theorem. This is not true for the normalized skewness, that measures the fluctuation asymmetry induced by the current. In this regime, the skewness opens the possibility to measure the carrier charge $e = e$ that is no more addressable via the Fano factor. Indeed, for low voltages $V \ll 0^+$ one has

$$k_3 = 2 - 1 - 3 \frac{1}{(1 + \gamma^2 C \cosh^2(E_c(\phi - 1=2)))} ; (6)$$

that does depend on ϕ but not on the exponent g .

We study now higher voltages $eV > 2E_c$ where the renormalized interaction parameter g has a prominent role. For this purpose we consider the behaviour of the Fano factor. Here in general a numerical approach is necessary. In Fig. 3 a density plot of k_2 for $g = 1=3$ as a function of magnetic field and source-drain voltage is shown for different asymmetries. We recover that, independently from ϕ , in region I one has $k_2 =$ that corresponds to a poissonian statistics. We will thus refer to the red (blue) regions, where $k_2 > (<)$, as super(sub)-poissonian noise regimes.

In the three-state regime III, a comparison of the top and bottom panels shows that super-poissonian values are induced by high barrier asymmetry. The Fano factor in this regime depends on a larger set of rates $\Gamma^n = (\Gamma^n)$, $n = 0;1$, and the corresponding backward rates $\Gamma^{-n} = e^{-\Gamma^n}$. A tractable analytical formula can be derived under the reasonable assumption that only two backward rates, Γ^{-0} and Γ^{-1} , survive: one has $k_2 = 1 - 2 \frac{\Gamma^{-1}}{\Gamma^{-0} + \Gamma^{-1}}$.

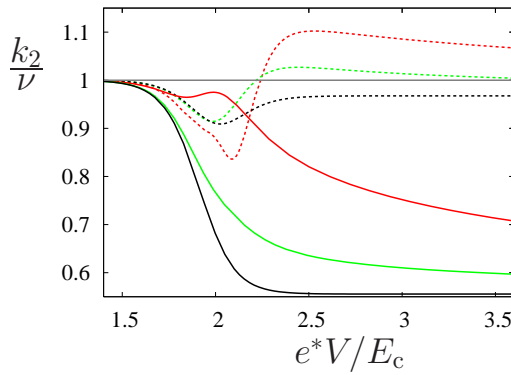


FIG. 4: Fano factor $k_2 =$ vs. $eV = E_c$ at $\eta' = 0$; $k_B T = 0.05 E_c$. Color code: red $g = 1/3$, green $g = 0.8$, black $g = 1$. Solid lines $\eta = 1$, dashed lines $\eta = 10$. Grey line, poissonian limit.

with

$$k_2 = \frac{0^2 + 1 + 1 + 1^2 + 0 + 0 + 0 + 1 + 0 + 1}{0 + 1 + 0 + 1 + 1 + 1 + 2} : \quad (7)$$

Here, $\frac{0}{t} = \frac{0}{+} + \frac{-0}{+}$ and $\frac{1}{t} = \frac{1}{+} + \frac{-1}{+}$. We note that in order to have super-poissonian noise a fractional $g < 1$ is necessary, with additional conditions on the asymmetry. Indeed, setting $\eta = 1$ in Eq. (7) in the limit E_+^1 ; $E_-^0 = 1$ yields $k_2 > 0$ for any g . On the other side, setting $g = 1$ gives $k_2 = 2 = (1^2 + 1 + 1)^2 > 0$. So it appears that positive correlations are induced by an interplay of η and g . Figure 4 shows the Fano factor as a function of $eV = E_c$ for different η and g . Here $\eta' = 0$, although similar considerations apply in general. For $g = 1$, k_2 remains sub-poissonian (black lines), while positive correlations appear for $g < 1$ and sufficient asymmetry (color lines).

Finally, interesting effects take place in the ν -state regime (V) for $\eta = 1/3$. Here, a superpoissonian Fano factor appears along the diamond lines for $\eta = 1$ (see Fig. 3 top) and disappears for large asymmetries (Fig. 3 bottom). Detailed investigations [23] show that the collective excitations of the antidot edge are responsible of the super-poissonian behaviour at small asymmetries. In this region, in fact, the tunneling process can excite the plasmonic modes of energy $\epsilon = 2E_c$ that exactly correspond to the diamond lines (Fig. 1(b), thick curves). In particular, one can show [23] that k_2 shows a superpoissonian maximum as a function of eV with a peculiar scaling law $k_2^{\text{max}} / T^{g-1}$ directly connected to the renormalized lead exponent.

In conclusion, we have found distinct, unambiguous signatures of fractional charge and interaction renormalization in high moments of tunneling current in a promising Hall-antidot geometry [11]. Confirmation of such novel results appears to be within experimental reach,

especially on account of recent accomplishments in measurement techniques applied to electron counting [24].

Financial support by the EU via Contract No. M CRTN-CT 2003-504574 is gratefully acknowledged.

-
- [1] R. B. Laughlin, Phys. Rev. Lett. 50, 1395 (1983).
 - [2] X. G. Wen, Phys. Rev. Lett. 64, 2206 (1990); Phys. Rev. B 41, 12838 (1990); 43, 11025 (1991).
 - [3] C. L. Kane and M. P. A. Fisher, Phys. Rev. Lett. 72, 724 (1994).
 - [4] R. de Picciotto, M. Reznikov, M. Heiblum, V. Umansky, G. Bunin, and D. Mahalu, Nature (London) 389, 162 (1997); L. Saminadayar, D. C. Glatelli, Y. Jin, and B. Etienne, Phys. Rev. Lett. 79, 2526 (1997).
 - [5] A. M. Chang, L. N. Pfeiffer, and K. W. West, Phys. Rev. Lett. 77, 2538 (1996); M. Grayson, D. C. Tsui, L. N. Pfeiffer, K. W. West, and A. M. Chang, ibid. 80, 1062 (1998).
 - [6] S. Roddaro, V. Pellegrini, F. Beltram, G. Biasiol, and L. Sorba, Phys. Rev. Lett. 93, 046801 (2004).
 - [7] B. Rosenow and B. I. Halperin, Phys. Rev. Lett. 88, 096404 (2002).
 - [8] O. Heinonen and S. Eggert, Phys. Rev. Lett. 77, 358 (1996).
 - [9] V. Ponomarenko and N. Nagaosa, Phys. Rev. B 60, 16865 (1999).
 - [10] K. Yang, Phys. Rev. Lett. 91, 036802 (2003).
 - [11] V. J. Goldman, Jun Liu, and A. Zaslavsky, Phys. Rev. B 71, 153303 (2005); V. J. Goldman, I. Karakurt, Jun Liu, and A. Zaslavsky, ibid. 64, 085319 (2001).
 - [12] M. R. Geller and D. Loss, Phys. Rev. B 56, 9692 (1997).
 - [13] A. Furusaki, Phys. Rev. B 57, 7141 (1998).
 - [14] M. R. Geller and D. Loss, Phys. Rev. B 62, R16298 (2000).
 - [15] A. Braggio, R. Fazio, and M. Sassetti, Phys. Rev. B 67, 233308 (2003).
 - [16] L. S. Levitov and M. Reznikov, Phys. Rev. B 70, 115305 (2004).
 - [17] H. Sakur and U. Weiss, Phys. Rev. B 63, 201302(R) (2001).
 - [18] In the point contact geometry the tunneling limit is a special regime, with Poissonian statistics e.g. for both $\eta = 1$ and $\eta = 1/3$.
 - [19] D. A. Bagrets and Yu. V. Nazarov, Phys. Rev. B 67, 085316 (2003).
 - [20] N. Byers and C. N. Yang, Phys. Rev. Lett. 7, 46 (1961).
 - [21] Y. M. Blanter and M. Buttiker, Phys. Rep. 336, 1 (2000).
 - [22] An analytical approximation for the minimum is given by $\eta^{\text{min}} = 1/2$ ($eV = 4E_c$) $(1 - \eta^{(g)}) = (1 + \eta^{(g)})$, with $\eta = [1 + O(E_c)]$.
 - [23] A. Braggio, M. Merlo, N. Magnoli, and M. Sassetti (unpublished).
 - [24] Yu. Bomze, G. Gershon, D. Shovkun, L. S. Levitov, and M. Reznikov, Phys. Rev. Lett. 95, 176601 (2005); S. Gustavsson, R. Leturcq, B. Simovic, R. Schleser, T. Ihn, P. Studerus, K. Ensslin, D. C. D. Riscoll, and A. C. Gossard, cond-mat/0510269.